



COMPUTER SIMULATION ON DYNAMIC SOIL-STRUCTURE INTERACTION SYSTEM

Peizhen Li¹, Xilin Lu², Bo Chen³ and Yueqing Chen⁴

SUMMARY

Three-dimensional finite element analysis in time domain on dynamic soil-structure interaction of a practical engineering is carried out in this paper. General-purpose finite element program ANSYS is used in the analysis. Commonly used equivalent linearity model is chosen as constitutive relation of soil. Viscous boundary of soil is implemented in ANSYS program. The influences of parameters are discussed, such as soil property and the rigidity of structure, excitation, on dynamic characteristics, seismic response and interaction effect of SSI system.

In order to analyze the effect of the liquefaction of sand on the seismic response of the SSI system, the effective stress method of considering the soil as equivalent linear material in every time interval is introduced in this paper. The above procedure is realized in ANSYS program by using the ANSYS Parametric Design Language (APDL). The earthquake response of sand-pile-high-rise building is analyzed, and the analysis results show the liquefaction of sand has large effect on the seismic response of structure in sand-pile-structure interaction system.

Key Words: Computer simulation, Soil-structure interaction, ANSYS program, Liquefaction, Seismic response.

INTRODUCTION

Over the last 40 years, the dynamic Soil-Structure Interaction (SSI) has attracted an intensive interest among researchers and engineers in the fields of structural dynamics, wave mechanics and soil dynamics over the world. The methods of their investigations include experimental study and analysis research. The analysis methods are generally classified into two kinds, analytical method and numerical simulation methods. Due to the underdevelopment of computer technology, analytical method was popular in the 1970's. However, the analytical method can only be used to solve simple problems. Along with the rapid

¹ Lectuer, State Key Lab. for Disaster Reduction in Civil Eng., Tongji Univ., Shanghai, 200092, China.

² Professor, State Key Lab. for Disaster Reduction in Civil Eng., Tongji Univ., Shanghai, 200092, China.
Email: lx1st@mail.tongji.edu.cn

³ Engineer, Office of Guangzhou Construction Science & Technology Committee, Guangzhou, 510030, China.

⁴ Associate Professor, Institute of Civil Eng., Wuhan Univ., Wuhan, 430072, China.

progress in the art of computer science, now numerical simulation methods are widely used to the study on SSI. Numerical simulation methods are roughly sorted into three kinds, such as substructure method (Chopra [1]), finite element method and hybrid method (Toki [2]). Substructure method is commonly applied to linear analysis due to the use of the superposition principle. Finite element method is applicable for most complex cases. Hybrid method can be considered as the integrating of analytical method and numerical method, or the integrating of different numerical methods in different fields, which can take full advantage of these methods.

Three-dimensional finite element analysis on a practical engineering considering SSI is carried out in this paper. In the computer simulation on SSI system, the nonlinear behavior of layered soil is simulated with the commonly used equivalent linearity model, and viscous boundary is adopted as boundary of soil. A computational method of investigation on practical engineering considering SSI by general-purpose finite element program ANSYS is explored in this paper, which is of great advantage to the popularization of SSI study and promote the study outcomes to guide practical engineering.

Furthermore, in order to analyze the effect of the liquefaction of sand on the seismic response of the pile and the superstructure, the effective stress method of considering the soil as equivalent linear material in every time interval is introduced in this paper. The above procedure is realized in ANSYS program by using the APDL, and earthquake response of sand-pile-high-rise building is analyzed. The calculation results show that the liquefaction of sand has large effect on the seismic response of structure in sand-pile-structure interaction system.

THREE-DIMENSIONAL FINITE ELEMENT ANALYSIS ON SSI SYSTEM

Combining general-purpose finite element program ANSYS, three-dimensional finite element analysis on SSI system has been carried out. The rationality of the modeling method has been verified in previous study by comparison analysis between the calculation and the shaking table model tests (Lu [3]).

Brief Description of a Practical Engineering

A cast-in-place frame structure supported on pile-raft foundation is studied in this paper. The layout of column grid is shown in Fig.1. The frame structure has 12 stories aboveground and one story underground. The height of underground floor is 2.8m, while the height of ground floor is 4.5m and the height of other floors is 3.6m. The thickness of cast-in-place floorslab is 120mm, the dimensions of column, boundary beam, and walkway beam are 600×600 mm, 250×600 mm, and 250×400 mm, respectively. The raft thickness of pile-raft foundation is 0.8m, the dimension of pile is 450×450 mm, and the length of pile is 39m with 0.7m entering the bearing stratum. The layout of pile-raft foundation is shown in Fig.2. The deformed bar of grade II (The yield strength f_y is 340MPa) is used as main reinforcement, and the concrete grade is C30 (The compressive strength f_c ' is about 21MPa).

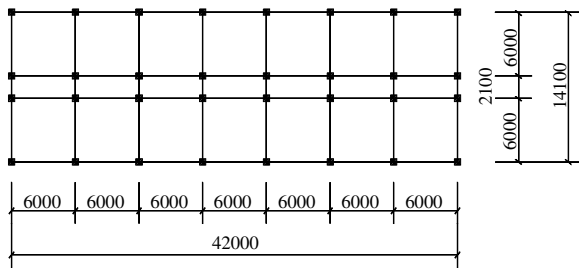


Fig.1 Layout of Column Grid

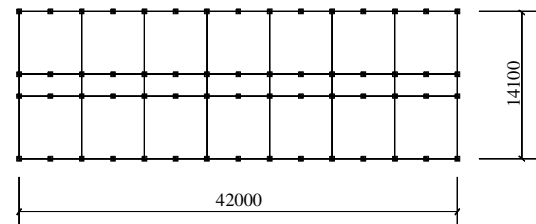


Fig.2 Layout of Pile-Raft Foundation

The distribution of soil near the First Shimen Road of Shanghai is used (DGJ08-11-1999 [4]). According to the classification of soil category defined in Shanghai local foundation design code of DGJ08-11-1999, the layers of soil from top to bottom are ①fill, ③very soft gray silty clay, ④very soft gray clay, ⑤₋₁ gray clay, ⑤₋₂gray silty clay, ⑤₋₃terreverte clay, ⑦strawyellow-gray silty sand. The shear wave velocity and mass density of soil are shown in Table 1.

Dynamic Constitutive Model of Soil

In this paper, equivalent linearization model of soil is adopted to simulate the material nonlinearity of soil. Based on the relationships of $G_d - \gamma_d$ and $D - \gamma_d$, a set of G_d , D and γ_d is obtained harmoniously by iteration. $G_d - \gamma_d$ denotes the relationship between dynamic shear modulus G_d and dynamic shear strain γ_d , while $D - \gamma_d$ denotes the relationship between damping ratio D and dynamic shear strain γ_d .

The soil's skeleton curve of Davidenkov model is adopted in this paper, and the relationship of $G_d/G_{\max} - \gamma_d$ is shown as Equation 1.

$$\frac{G_d}{G_{\max}} = 1 - H(\gamma_d) \quad (1)$$

$$H(\gamma_d) = \left[\frac{(|\gamma_d|/\gamma_r)^{2B}}{1 + (|\gamma_d|/\gamma_r)^{2B}} \right]^A \quad (2)$$

$$G_{\max} = \rho V_s^2 \quad (3)$$

$$\gamma_r = \gamma'_r (0.01 \sigma'_0)^{1/3} \quad (4)$$

G_{\max} is the maximum dynamic shear modulus of soil, ρ is the mass density of soil, and V_s is the shear wave velocity of soil. γ_r is a shear strain for reference. σ'_0 is the average effective confining pressure of soil, and its unit is kPa . The values of parameter A , B and γ'_r are shown in Table 2.

The hysteresis loop of soil $D/D_{\max} - \gamma_d$ is expressed as following empirical formula.

$$\frac{D}{D_{\max}} = (1 - \frac{G_d}{G_{\max}})^{\beta} \quad (5)$$

D_{\max} is the maximum damping ratio of soil. β is the shape factor of curve $D/D_{\max} - \gamma_d$, and 1.0 is chosen as β for soft soil of Shanghai area. The value of D_{\max} is reference to Table 2.

Table 1 Soil Property

| No. | Bottom Depth (m) | Mass Density (kg/m ³) | Shear Wave Velocity (m/s) |
|-----------------|------------------|-----------------------------------|---------------------------|
| ① | 3.5 | 1800 | 90 |
| ③ | 8.0 | 1740 | 140 |
| ④ | 17.6 | 1700 | 140 |
| ⑤ ₋₁ | 26.5 | 1770 | 160 |
| ⑤ ₋₂ | 35.2 | 1810 | 180 |
| ⑤ ₋₃ | 41.3 | 1990 | 210 |
| ⑦ | >41.3 | 1960 | >210 |

Table 2 Parameter of Davidenkov Model for Shanghai Soil

| Soil Type | A | B | D_{\max} | γ'_r (10^{-3}) |
|--------------------|------|------|------------|------------------------------|
| clay | 1.62 | 0.42 | 0.30 | 0.6 |
| silt | 1.12 | 0.44 | 0.25 | 0.8 |
| sand soil | 1.10 | 0.48 | 0.25 | 1.0 |
| medium coarse sand | 1.10 | 0.48 | 0.25 | 1.2 |

In ANSYS program, there is a kind of parametric design language named APDL, which is a scripting language. Users can use it to automate common tasks or even build models in terms of parameters. The equivalent linearity model is realized in ANSYS program by using the APDL, and the calculation of material nonlinearity is realized automatically.

Viscous Boundary of Soil

The use of finite element method for SSI study dictates that the infinite medium is truncated along certain boundaries (called artificial boundaries) and thus is reduced to a finite region (called near field). In order to have meaningful results, the artificial boundaries, which actually do not exist, can transmit waves from near to far field without reflections, or at least the wave reflections back into near field can be ignored. The artificial boundary conditions may be also interpreted as the constitutive equations for the interaction forces between near and far fields; thus their performance in SSI analysis depends on how correctly they describe these forces.

The artificial boundary conditions can be classified as viscous boundary, superposition boundary, paraxial boundary, extrapolation boundary and so on (Lysmer [5]) (Lysmer [6]) (White [7]). The viscous boundary is the most commonly used boundary conditions in practice as it has a simple form suitable for finite element formulation and nonlinear analysis. The viscous boundary is adopted in this paper.

Viscous boundary is equivalent to setting a series of dampers on artificial boundary to absorb wave energy. The damping coefficients of dampers have no relation to frequency. In this paper, viscous boundary is implemented by spring-damper element in ANSYS program. By using symmetry principle, the meshing of above practical engineering considering SSI is shown in Fig.3. Earthquake wave is inputted along transverse direction of the structure. Tenfold transverse size of structure is chosen as soil size, and viscous boundary is put on transverse boundary of soil. The viscous boundary is not drawn in Fig.3 in order to see the meshing clearly.

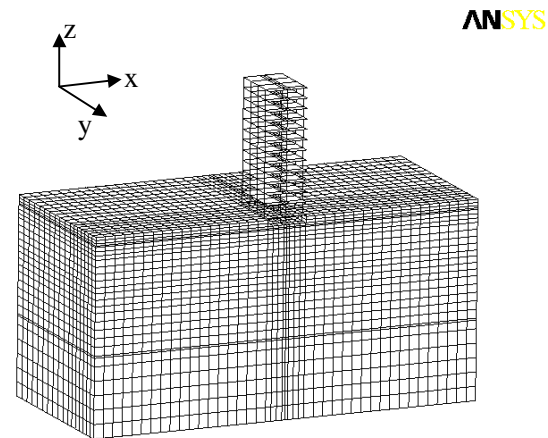


Fig.3 Meshing of SSI System

El Centro earthquake record, whose peak values of acceleration is adjusted to 0.1g, is inputted from the bottom of soil along X axis. In order to analyze the effect of the viscous boundary of soil, the computational analysis is carried out under following three conditions in this paper. ① Thirtyfold transverse size of structure is chosen as soil size, and free boundary is put on transverse boundary of soil. ② Tenfold transverse size of structure is chosen as soil size, and viscous boundary is put on transverse boundary of soil. ③ Tenfold transverse size of structure is chosen as soil size, and free boundary is put on transverse boundary of soil.

The plane center of ground floor is chosen as origin of coordinates. The comparison of displacement response between the above-mentioned condition ② and condition ① is shown in Fig.4. Above-mentioned condition ① is considered as infinite field in half space approximately. Point A13 in Fig.4 is the central point on the top of structure, and its elevation is 44.1m. Point CX1 is on the surface of soil intersection with structure, and its coordinate is (7.05, 0, -0.6). Figure 4 shows that the displacement time-history curves of corresponding points are approximately coincident. This conclusion can also be drawn from the comparison between other corresponding points in the soil-pile-structure system.

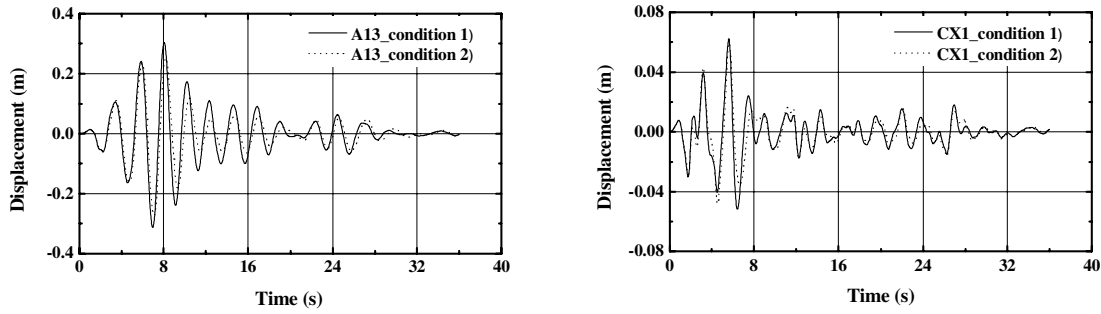


Fig.4 Comparison of Displacement Response

Table 3 shows the comparison of displacement peak value of points on soil surface along vibration direction between the above-mentioned three conditions. It shows that there is small difference between results under condition ② and condition ①, while the difference between results under condition ③ and condition ① is much larger. Therefore the size of computational model and computer resource can be reduced greatly by using viscous boundary, and the computational accuracy is still assured.

Table 3. Displacement Peak Value of Points on Soil Surface along Vibration Direction

| Coordinate X (m) | Condition ① | Condition ② | | Condition ③ | |
|---------------------|--------------------------------------|--------------------------------------|--------------------|--------------------------------------|--------------------|
| | Peak Value of Displacement (m) | Peak Value of Displacement (m) | Error to 1) (%) | Peak Value of Displacement (m) | Error to 1) (%) |
| 7.05 | 0.06229 | 0.06154 | -1.20179 | 0.07664 | 23.04647 |
| 10.575 | 0.05964 | 0.05951 | -0.22941 | 0.07455 | 24.99032 |
| 14.1 | 0.05877 | 0.05893 | 0.27211 | 0.07415 | 26.15420 |
| 17.625 | 0.05819 | 0.05889 | 1.20171 | 0.07439 | 27.84853 |
| 21.15 | 0.05784 | 0.05886 | 1.76267 | 0.07471 | 29.16283 |
| 24.675 | 0.05757 | 0.05900 | 2.47840 | 0.07529 | 30.77701 |
| 28.2 | 0.05735 | 0.05921 | 3.23780 | 0.07600 | 32.50813 |
| 31.725 | 0.05721 | 0.05949 | 3.97624 | 0.07683 | 34.28527 |
| 35.25 | 0.05704 | 0.05982 | 4.86760 | 0.07777 | 36.33333 |

Input Excitation

El Centro record and Shanghai artificial wave is adopted as input excitation. Frequency content of these two seismic waves is shown in Fig.5 and Fig.6.

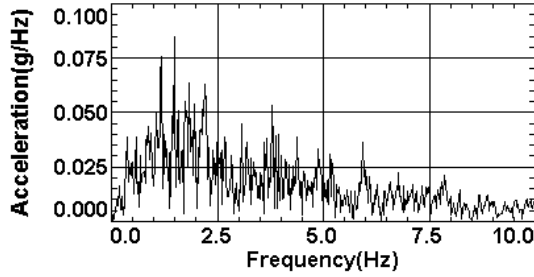


Fig.5 Frequency Content of El Centro

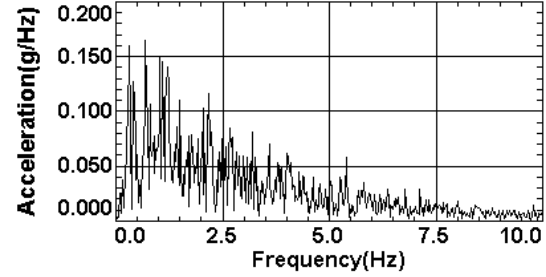


Fig.6 Frequency Content of Shanghai artificial

SSI Study on Different Soil Properties

Suppose the equivalent dynamic shear modulus of above-mentioned soil of Shanghai area after iteration is G . Three-dimensional finite element calculation on SSI with different soil properties, such as $0.2G$, $0.5G$, $1G$, $2G$, $3G$ and $5G$, is carried out. $0.2G$, $0.5G$, $1G$, $2G$, $3G$ and $5G$ denote that the dynamic shear modulus of soil are 0.2, 0.5, 1, 2, 3 and 5 times of G , respectively. El Centro earthquake record, whose peak values of acceleration is adjusted to $0.1g$, is inputted from the bottom of soil along X axis.

Natural frequency

Table 4 shows the natural frequency of SSI system of different soil properties. It is clear that natural frequency increases along with the increase of the dynamic shear modulus of soil, and furthermore, the increment of higher order is larger than that of lower order. The natural frequency of SSI system is lower than that of structure supported on rigid ground, that is to say, the natural frequency of the structure system decreases and period increases under consideration of SSI.

Table 4 Natural Frequency of SSI System with Different Soil Properties

| No. | A: 0.2 <i>G</i> | | B: 1 <i>G</i> | C: 5 <i>G</i> | | D: Rigid Ground | |
|-----|-----------------|----------------|----------------|----------------|----------------|-----------------|----------------|
| | Frequency (Hz) | Error to B (%) | Frequency (Hz) | Frequency (Hz) | Error to B (%) | Frequency (Hz) | Error to B (%) |
| 1 | 0.202 | -52.3 | 0.423 | 0.471 | 11.3 | 0.507 | 19.7 |
| 2 | 0.290 | -38.3 | 0.471 | 1.017 | 115.9 | 1.580 | 235.4 |
| 3 | 0.321 | -51.2 | 0.658 | 1.458 | 121.7 | 2.845 | 332.5 |
| 4 | 0.364 | -49.4 | 0.719 | 1.525 | 112.1 | 4.224 | 487.6 |
| 5 | 0.407 | -54.1 | 0.888 | 1.607 | 81.0 | 5.783 | 551.3 |

Seismic response of structure

Fig.7 presents the acceleration peak value, displacement peak value, interstory shear and overturning moment of the structure. It is obvious that the seismic response of structure is very complicated along with the change of dynamic shear modulus of soil. By analysis of natural frequency of SSI system, it is found that participation of the first mode shape is most notable along the vibration direction when dynamic shear modulus is $0.2G$, while participation of the second mode shape enhances gradually along with the increase of dynamic shear modulus of soil.

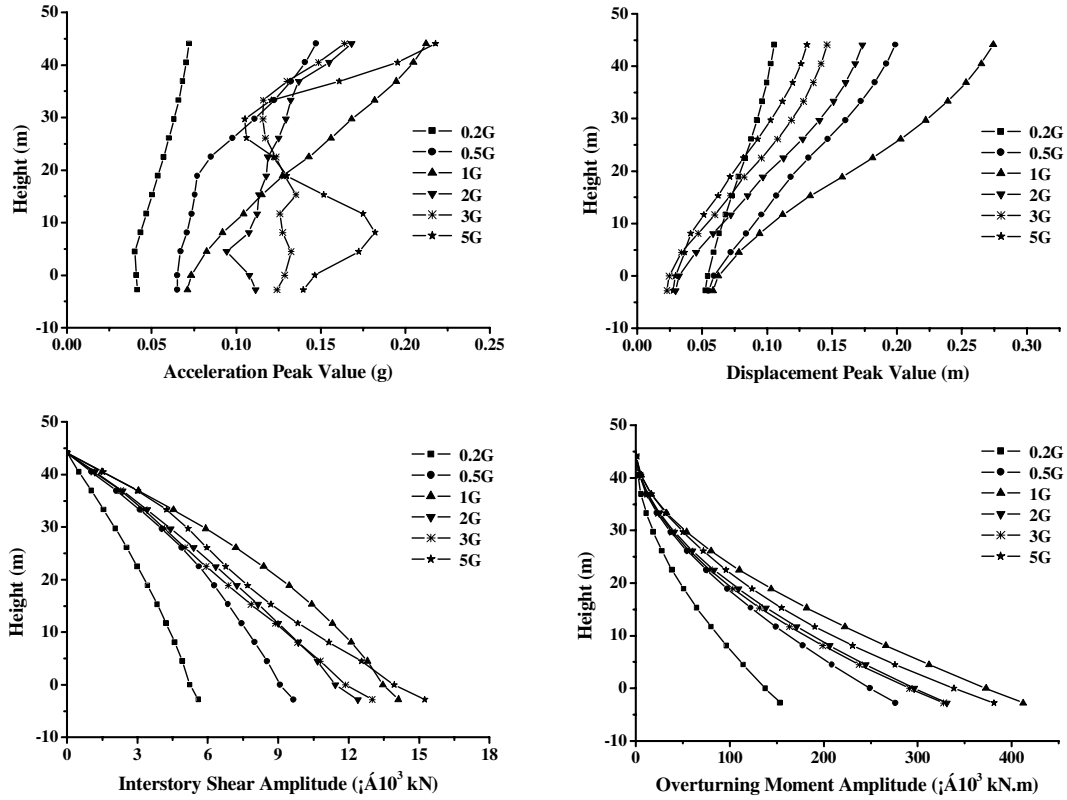


Fig.7 Seismic Response of Structure (Soil of Different Properties)

Effect of SSI on displacement peak value of structure supported by different soil

Table 5 indicates the effect of SSI on displacement peak value of the structure supported by soil with different properties. When SSI is not taken into account, the ground shock, which is inputted from structure bottom, is the acceleration time-history of surface point, adequately far away from the structure. Issues drawn from Table 5 are as follows. 1) Displacement peak value of the structure under consideration of SSI is commonly larger than that of the structure supported by rigid ground. 2) SSI has notable effect on displacement peak value of the structure at bottom part, while has less effect on displacement peak value of the structure at top part. 3) The effect of SSI on displacement peak value of the structure becomes larger along with the decrease of the shear modulus of soil.

Effect of SSI in Shanghai soft soil area

In Fig.8, the effect of SSI in Shanghai soft soil area on acceleration peak value, interstory drift, interstory shear and overturning moment of the structure are presented. From Fig.5, the acceleration peak value, interstory shear and overturning moment of the structure under consideration of SSI are smaller than those under condition of rigid ground, respectively. The maximum value of reduction is 10.4%, 8.2% and 7.7%, respectively. The interstory drift of the structure under consideration of SSI is larger than that under condition of rigid ground near the top of the structure, while less than that near the bottom of the structure.

The maximum change is 36.6%. The maximum of acceleration peak value is at the top of the structure, while maximums of interstory shear and overturning moment are at the bottom of structure. The maximum of interstory drift is between ground floor and the second floor above the ground floor, because the stiffness of underground floor is much larger than that of the ground floor.

**Table 5 Displacement Peak Value of Structure along Vibration Direction
(Different Soil Property)**

| Soil Property | A: 0.2G | | | B: 1 G | | | C: 5 G | | |
|---------------|---------|--------|---------|--------|--------|---------|--------|--------|---------|
| Height (m) | I (m) | II (m) | III (%) | I (m) | II (m) | III (%) | I (m) | II (m) | III (%) |
| -2.8 | 0.053 | 0 | -- | 0.059 | 0 | -- | 0.028 | 0 | -- |
| 0 | 0.054 | 0.002 | 2379 | 0.063 | 0.009 | 622 | 0.039 | 0.004 | 559 |
| 4.5 | 0.059 | 0.011 | 443 | 0.078 | 0.043 | 83.2 | 0.037 | 0.021 | 70.9 |
| 8.1 | 0.063 | 0.018 | 254 | 0.094 | 0.070 | 34.4 | 0.041 | 0.034 | 20.7 |
| 15.3 | 0.073 | 0.032 | 131 | 0.133 | 0.123 | 8.5 | 0.062 | 0.055 | 12.5 |
| 22.5 | 0.083 | 0.044 | 88.8 | 0.181 | 0.170 | 6.8 | 0.082 | 0.079 | 3.6 |
| 29.7 | 0.092 | 0.054 | 69.7 | 0.222 | 0.209 | 6.4 | 0.103 | 0.103 | 0.16 |
| 36.9 | 0.099 | 0.062 | 61.5 | 0.253 | 0.237 | 6.9 | 0.120 | 0.122 | -1.57 |
| 44.1 | 0.106 | 0.066 | 59.8 | 0.274 | 0.253 | 8.2 | 0.131 | 0.133 | -1.63 |

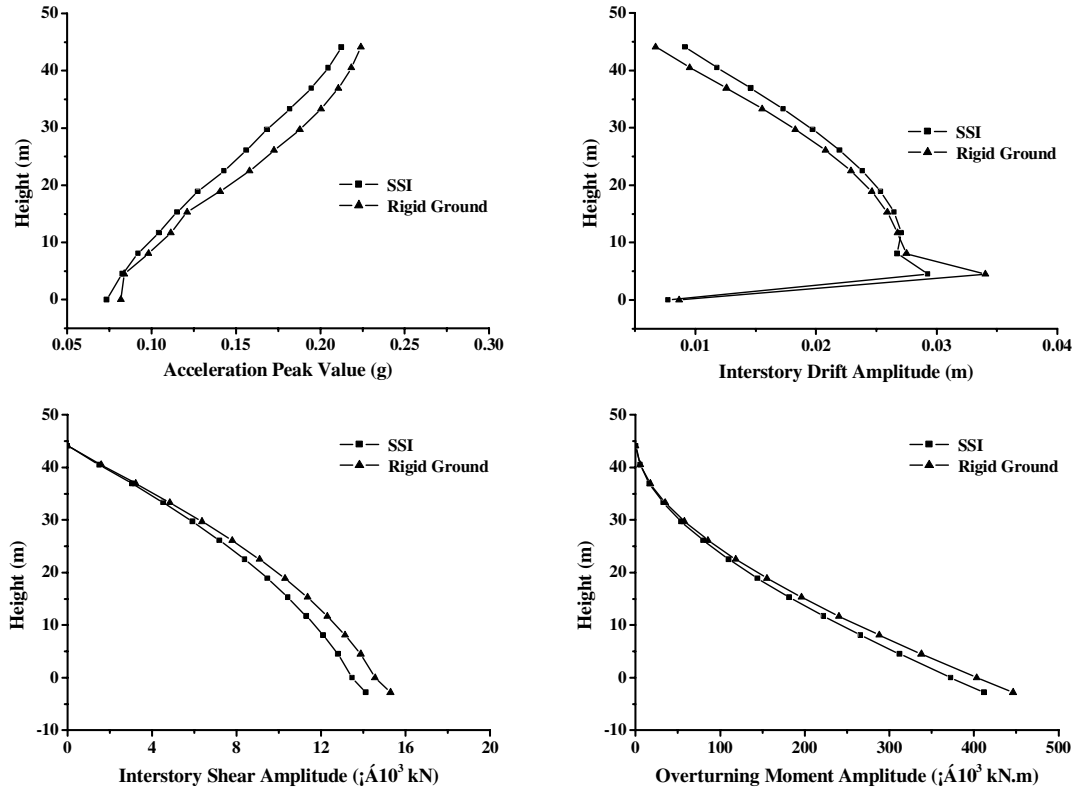


Fig.8 Seismic Response of Structure (Comparison between SSI and Rigid Ground)

Effect of SSI on Displacement Peak Value of Structure with Different Rigidity

Table 6 shows the effect of SSI on displacement peak value of the structure with different rigidity. The different rigidity of the structure is realized by adopting different grade of concrete. Issues drawn from Table 6 are as follows. 1) SSI has a notable effect on displacement peak value of the structure at bottom part, while has less effect on displacement peak value of the structure at top part. 2) The effect of SSI on displacement peak value of the structure is larger along with the increase of the structure rigidity.

**Table 6 Displacement Peak Value of Structure along Vibration Direction
(Different Concrete Grade)**

| Grade of Concrete | A: C20 | | | B: C30 | | | C: C40 | | |
|-------------------|--------|--------|---------|--------|--------|---------|--------|--------|---------|
| Height (m) | I (m) | II (m) | III (%) | I (m) | II (m) | III (%) | I (m) | II (m) | III (%) |
| -2.8 | 0.056 | 0 | -- | 0.059 | 0 | -- | 0.058 | 0 | -- |
| 0 | 0.059 | 0.010 | 482 | 0.063 | 0.009 | 623 | 0.062 | 0.007 | 731 |
| 4.5 | 0.072 | 0.050 | 43.5 | 0.078 | 0.043 | 83.2 | 0.077 | 0.037 | 109 |
| 8.1 | 0.088 | 0.083 | 6.67 | 0.094 | 0.070 | 34.44 | 0.091 | 0.060 | 51.4 |
| 15.3 | 0.131 | 0.145 | -9.64 | 0.133 | 0.123 | 8.53 | 0.123 | 0.105 | 16.4 |
| 22.5 | 0.185 | 0.201 | -8.15 | 0.181 | 0.170 | 6.81 | 0.165 | 0.146 | 12.9 |
| 29.7 | 0.231 | 0.247 | -6.51 | 0.222 | 0.209 | 6.40 | 0.201 | 0.179 | 11.8 |
| 36.9 | 0.266 | 0.279 | -4.79 | 0.253 | 0.237 | 6.94 | 0.228 | 0.203 | 12.1 |
| 44.1 | 0.289 | 0.298 | -3.10 | 0.274 | 0.253 | 8.25 | 0.246 | 0.217 | 13.3 |

Note: I -- Displacement peak value of structure under consideration of SSI;

II -- Displacement peak value of structure without consideration of SSI;

III -- Relative error between I and II, namely $III=(I-II)/II*100\%$.

Seismic Response of Structure under Different Excitation

Fig.9 displays the acceleration peak value, displacement peak value, interstory shear and overturning moment of the structure under excitation of El Centro wave and Shanghai artificial wave. The acceleration peak values of El Centro wave and Shanghai artificial wave are both adjusted to 0.1g. It shows that the seismic response of structure under the excitation of Shanghai artificial wave is obviously bigger than that under the excitation of El Centro wave. The main reason is that the low frequency of Shanghai artificial wave is very abundant, and the frequency of SSI system is very low.

TWO-DIMENSIONAL EFFECTIVE STRESS ANALYSIS ON SSI SYSTEM

Constitutive Model of Soil

In this paper, Drucker-Prager model is adopted as static constitutive model of sand. And the soil's skeleton curve of Davidenkov model is applied as dynamic constitutive model of soil. As shown in Fig. 10, the dynamic shear modulus and shear intensity of saturated soil declined under excitation of cycle load. The decline may be caused by increasing of pore water pressure and can be described by decreasing

the G_{max} and τ_{max} . Supposing the decreased maximum shear modulus and shear intensity as G_{mt} and τ_{mt} , then:

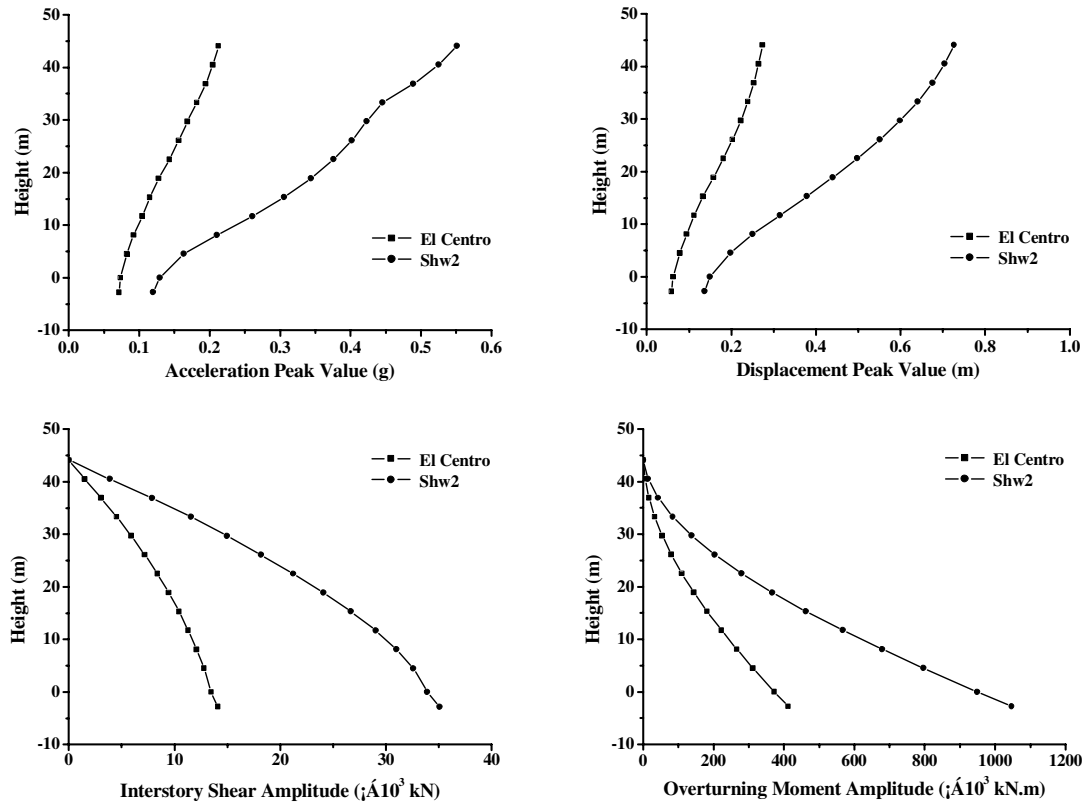


Fig.9 Seismic Response of Structure (Comparison between El Centro and Shanghai Wave)

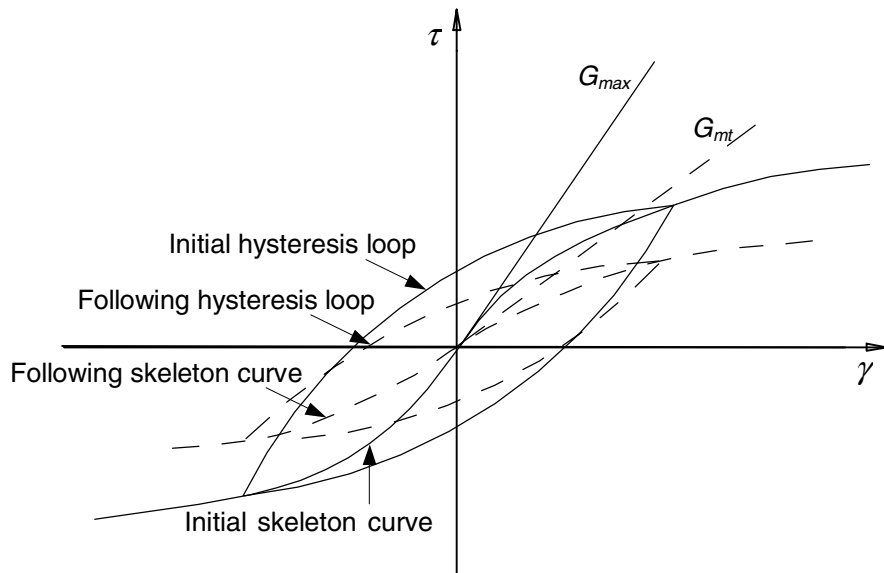


Fig. 10 Stress-strain curve under excitation of cyclic load

$$G_{mt} = G_{\max} (1 - u^*)^{\frac{1}{2}} \quad (6)$$

$$\tau_{mt} = \tau_{\max} (1 - (u^*)^v) \quad (7)$$

u^* is the pore water pressure ratio. v is a constant and the value of v is usually taken as 3.5~5.0.

The hysteresis loop of soil $D/D_{\max} - \gamma_d$ is expressed as following empirical formula.

$$\frac{D}{D_{\max}} = (1 - \frac{G}{G_{mt}})^{\beta} \quad (8)$$

D_{\max} is the max damping ratio of soil. β is the shape factor of curve $D/D_{\max} - \gamma_d$, and 1.0 is chosen as β for soft soil of Shanghai area. The value of D_{\max} is reference to Table 2.

Pore Water Pressure Mode of Sand Soil

The increment mode of pore water pressure of Shanghai sand soil could be expressed as follows:

$$u^* = u / \sigma'_0 = (1 - m\alpha_s) 2 / \pi \arcsin(N / N_f)^{1/2\theta} \quad (9)$$

$$\Delta u^* = \frac{\Delta u}{\sigma'_0} = \frac{(1 - m\alpha_s) \Delta N}{\pi \theta N \sqrt{1 - (N / N_f)^{1/\theta}}} \left(\frac{N}{N_f} \right)^{1/2\theta} \quad (10)$$

Δu is pore water pressure induced by seismic vibration within the time of ΔT .

σ'_0 is initial average effective stress.

m is a constant from test, and the value is usually taken between 1.0 and 1.2.

α_s is the level of static stress, and can be figured out by equation 12.

ΔN is equivalent vibration times in every time interval, and can be figured out by equation 15.

N is total vibration times, and $N = \sum \Delta N$.

θ is a constant, and Seed deems that 0.7 can be chosen as the value for most soil.

N_f is the vibration times when liquefaction occur. And it can be calculated from equation 11.

$$aN_f^{-b} = \tau_d / \sigma'_0 \quad (11)$$

τ_d is peak value of cycle shear stress. a and b are constant from test.

Assuming the destroyed area is the maximum cycle shear area under plain strain state, initial static shear ratio α_s and dynamic shear stress ratio α_d can be drawn from following equations (Chen, [8]).

$$\alpha_s = 2 \left| \tau_{xy} \right| / \sqrt{(\sigma'_x + \sigma'_y + 2\sigma'_c)^2 - 4\tau_{xy}^2} \quad (12)$$

$$\alpha_d = \frac{\tau_d}{\sigma'} = \frac{2|\tau_{xy,d}|}{\sqrt{(\sigma'_x + \sigma'_y + 2\sigma_c)^2 - 4\tau_{xy}^2} + |\sigma'_x - \sigma'_y|} \quad (13)$$

σ'_x , σ'_y and τ_{xy} is static normal effective stress and static shear stress on horizontal area, respectively.

$\sigma_c = c' \cdot \text{ctg} \varphi'$, c' and φ' is cohesive strength and internal friction angle, respectively. The value of c' is zero for pure sand soil. $\tau_{xy,d}$ is equivalent cycle peak value of seismic shear stress on horizontal area.

ΔN is equivalent vibration times in every time interval, and can be figured out as follows. First, the duration time T_d and the effective vibration time N_{eq} is looked up in Table 7. Then, the ratio between energy of the seismic wave in time interval of ΔT_i and the corresponding energy in the whole duration time T_d is calculated:

$$SA(\Delta T_i) = \int_{t_{i-1}}^{t_i} a^2(t) dt \bigg/ \int_0^{T_d} a^2(t) dt \quad (14)$$

$$\Delta N = N_{eq} \cdot SA(\Delta T_i) \quad (15)$$

Dynamic analysis method with effective stress by step by step iteration in every time interval.

The analysis method is shown in detail as follows.

(1) The static effective stress σ'_x , σ'_y and τ_{xy} are worked out through static analysis. (2) The whole period of the seismic wave is divided into some equal intervals. The initial dynamic shear modulus and the initial damping ratio are determined for each of element. And analysis using the above-mentioned dynamic constitutive model of sand soil is carried out by step by step iteration method in the first time interval. (3) ΔN in this time interval and the accumulative value N are figured out. (4) Δu^* in this time interval and the accumulative value u^* are figured out using equation 9 for each of element. (5) G_{mt} and D_{mt} considering the effect of the pore water pressure are figured out for each of element. And the calculated value is used as the initial value for the next time interval. (6) Using the restart function of ANSYS program, the dynamic shear modulus and damping ratio are changed into the value worked out in the step (5). And the calculation of next time interval is carried out without exiting the program. In this way, the continuity of result can be ensured. The above step (2)~(6) should be repeated for each of time interval until the seismic wave finishes.

The magnitude of time interval has an effect on the calculation result. Reasonable magnitude of time interval relates with the site condition and the property of inputted seismic wave. Generally, the pore water pressure should have at least one whole cycle in each time interval.

DYNAMIC ANALYSIS OF SAND-PILE-TALL BUILDING SYSTEM CONSIDERING SAND LIQUEFACTION

Brief Description of a Practical Engineering

A cast-in-place frame structure supported on pile-raft foundation is studied in this paper. The layout of column grid is shown in Fig.1. The frame structure has 16 stories aboveground and one story underground. The height of underground floor is 2m, while the height of ground floor is 4m and the height of other floors is 2.8m. The dimensions of column, boundary beam, and walkway beam are $600 \times 600\text{mm}$, $250 \times 600\text{mm}$, and $250 \times 400\text{mm}$, respectively. The raft thickness of pile-raft foundation is 1.0m, the dimension of pile is $450 \times 450\text{mm}$, and the length of pile is 43m. The layout of pile-raft foundation is shown in Fig.2. The ground soil is uniform saturated sand and is 70 meters in thickness, which is on the top of the bedrock. The constitutive model of soil, the equation of damping and some other parameters in the calculation can refer to corresponding item mentioned above. The soil and pile are simulated by two-dimensional plain strain element. The column and beam are simulated by two-dimensional beam element. Simple truncation boundary, which is 60 meters far from the structure, is used as the lateral boundary. El Centro record is applied as inputted excitation. And the peak value is adjusted to 0.3g. One second is taken as the time interval.

Table 7 The value of N_{eq} and T_d

| Earthquake Magnitude | N_{eq} (time) | T_d (second) |
|----------------------|-----------------|----------------|
| 5.5~6 | 5 | 8 |
| 6.5 | 8 | 14 |
| 7 | 12 | 20 |
| 7.5 | 20 | 40 |
| 8 | 30 | 60 |

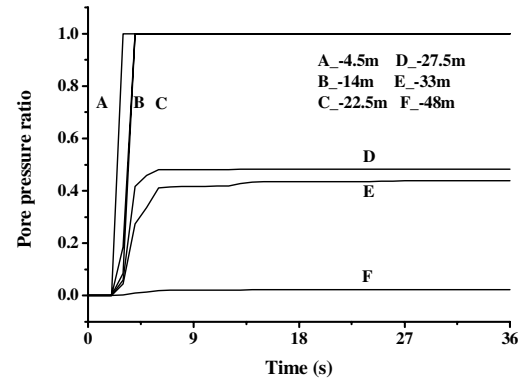


Fig.11 The increment curve of pore pressure ratio

The increment curve on pore water pressure ratio of sand soil is shown in Fig. 11. Liquefaction occurred at the third second in point 4.5m deep, and this phenomenon occurred at the fourth second in point 14~22.5m deep, while no liquefaction occurred in point 30~70m deep. Especially in sand at the top of pile, the pore water pressure ratio is smaller than 0.10.

The comparison of acceleration response between the effective stress method and general stress method is shown in Fig. 12. And the comparison of corresponding Fourier spectra is shown in Fig. 13. In the figure, “soil inner” is the point in soil among piles, which is 25m deep from surface of soil. And “soil surface” is on the surface of soil, which is 30m far away from the structure. It shows that the liquefaction and softening of ground soil could magnify low frequency wave and filter high frequency wave. Wave frequency higher than 5Hz are almost filtered. Having taken the affect of the pore water pressure into account in the effective stress method, the whole system becomes more flexible comparing with that in the general stress method. The effect of wave filter on high frequency become more evidently and the

peak value of Fourier spectrum curve move to lower frequency. The peak value of acceleration response of the “soil inner” and “soil surface”, which is calculated from the effective stress method, is 10% smaller than that from the general stress method. The peak value of acceleration response of the ground floor and the top floor is 10% and 17% smaller than that from the general stress method, respectively. Because liquefaction occurs in the soil near the surface at the third second and the seismic wave can not be transferred any more, the acceleration response on the surface of the ground soil becomes very small after the third second. The acceleration response of the super structure diminishes gradually after liquefaction occurs in most of soil. The acceleration response of the “soil inner” point keeps large because liquefaction does not occur in this point.

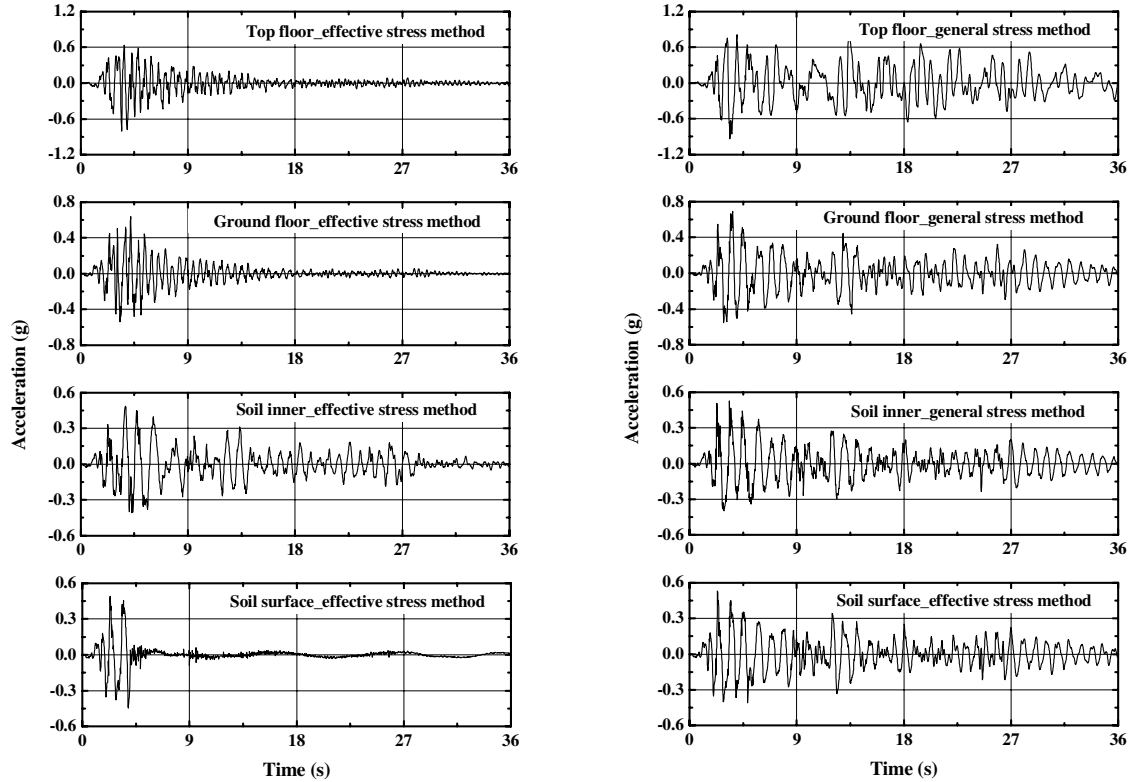


Fig.12 The comparison of acceleration response between the effective stress and general stress method

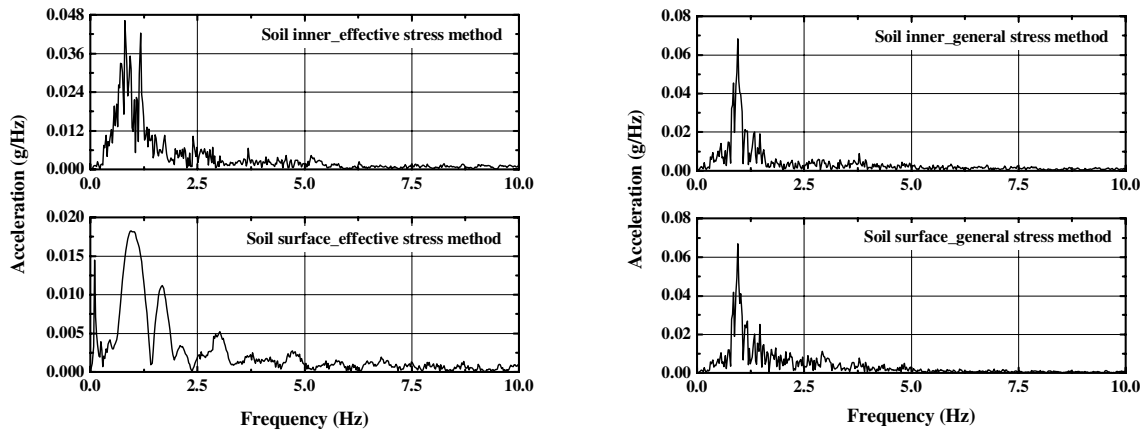


Fig.13 The comparison of acceleration Fourier spectra between the effective stress and general stress method

CONCLUSIONS

In this paper, combining general-purpose finite element program ANSYS, research on practical engineering considering SSI through both the general stress method and the effective stress method have been carried out, which is of great advantage to the popularization of SSI study and to the study outcomes to guide practical engineering. Issues drawn from the study are as follows. 1) Natural frequency of SSI system increases along with the increase of dynamic shear modulus of soil. 2) Seismic response of structure under consideration of SSI is very complicated along with the change of dynamic shear modulus of soil. 3) SSI has notable effect on displacement peak value of structure at bottom part, while has less effect on displacement peak value of structure at top part. 4) The effect of SSI on displacement peak value of structure becomes larger along with the decrease of shear modulus of soil. 5) The effect of SSI on displacement peak value of structure becomes larger along with increase of structure rigidity. 6) The liquefaction of sand has large effect on the seismic response of structure in sand-pile-structure interaction system.

ACKNOWLEDGEMENT

This project is carried out under the sponsorship of the key project (No.50025821) and the youth project (No.50308018) of National Natural Science Foundation of China.

REFERENCES

1. Chopra AK, Perumalswami PR. "Dam-foundation interaction during earthquakes." Proceedings of 4th World Conference Earthquake Engineering, Santiago, Chile. 1969.
2. Toki K, Sato T. "Seismic response analysis of surface layer with irregular boundaries." Proceedings of 6th World Conference On Earthquake Engineering, New Delhi, India. 1977.
3. Lu XL, Li PZ, Chen B, and Chen YQ. "Numerical Analysis of Dynamic Soil-Box Foundation-Structure Interaction System," Journal of Asian Architecture and Building Engineering, 2002; 1(2): 9-16
4. "Foundation Design Code (DGJ08-11-1999)." Shanghai, China, 1999.
5. Lysmer J, Kulemeyer RL. "Finite Dynamic Model for Infinite Media." J. Eng. Mech. Div., ASCE 1969; Vol.95: 759-877.
6. Lysmer J, Wass G. "Shear Waves in Plane Infinite Structures." J. Eng. Mech. Div., ASCE 1972; Vol.98: 85-105.
7. White W, Valliappan S, Lee IK. "Unified Boundary for Finite Dynamic Models." J. Eng. Mech. Div., ASCE 1977; Vol.103: 949-964.
8. Chen GX, Xie JF, Zhang KX. "Effect of Foundation Soil Liquefaction on Earthquake Response of Pile-supported High-rise Building System." Earthquake Engineering and Engineering Vibration 1995; 15(4): 93-103.